Journal of Solid State Chemistry 184 (2011) 3289–3298

Contents lists available at SciVerse ScienceDirect

Journal of Solid State Chemistry

journal homepage: www.elsevier.com/locate/jssc

Synthesis, crystal structure and magnetic characterization of metal(II) coordination polymers based on 2-carboxyethylphosphonic acid and 1,10-phenanthroline (metal=Cu, Co, Cd)

Eva Fernández-Zapico [a], Jose Manuel Montejo-Bernardo [a], Richard D'Vries [b], José R. García [a,*], Santiago García-Granda [a], Jesús Rodríguez Fernández [c], Imanol de Pedro [c], Jesús A. Blanco [d]

[a] Departamentos de Química Física y Analítica y Química Orgánica e Inorgánica, Universidad de Oviedo—CINN, 33006 Oviedo, Spain
[b] Instituto de Ciencias de Materiales de Madrid, CSIC, Cantoblanco, 28049 Madrid, Spain
[c] CITIMAC, Facultad de Ciencias, Universidad de Cantabria, 39005 Santander, Spain
[d] Departamento de Física, Universidad de Oviedo, 33007 Oviedo, Spain

ARTICLE INFO

Article history:
Received 27 May 2011
Received in revised form
26 September 2011
Accepted 3 October 2011
Available online 19 October 2011

Keywords:
Coordination polymers
Hydrothermal synthesis
Crystal structure
Magnetic characterization

ABSTRACT

Three non-isostructural metal(II) coordination polymers (metal=copper, cobalt, cadmium) were synthesized under the same mild hydrothermal conditions (T=408 K) by mixture of the corresponding metal acetate with 2-carboxyethylphosphonic acid and 1,10-phenanthroline (1:1:1 M ratio) and their structures were determined by single-crystal X-ray diffraction. $Cu_2(HO_3PCH_2CH_2COO)_2(C_{12}H_8N_2)_2(H_2O)_2$ and $Cd_2(HO_3PCH_2CH_2COO)_2(C_{12}H_8N_2)_2$ are triclinic (space group *P-1*) with a=7.908(5) Å, b=10.373(5) Å, c=11.515(5) Å, α=111.683(5)°, β=95.801(5)°, γ=110.212(5)° (T=120 K), and a=8.162(5) Å, b=9.500(5) Å, c=11.148(5) Å, α=102.623(5)°, β=98.607(5)°, γ=113.004(5)° (T=293 K), respectively. In contrast, $[Co_2(HO_3PCH_2CH_2COO)_2(C_{12}H_8N_2)_2(\mu\text{–}OH_2)](H_2O)$ is orthorhombic (space group *Pbcn*) with a=21.1057(2) Å, b=9.8231(1) Å, c=15.4251(1) Å (T=120 K). For these three compounds, structural features, including H-bond network and the π–π stacking interactions, and thermal stability are reported and discussed. None of the materials present a long-range magnetic order in the range of temperatures investigated from 300 K down to 1.8 K.

© 2011 Elsevier Inc. All rights reserved.

1. Introduction

Metal phosphonate chemistry is developing at a rapid growth in recent years, with a lot of new structures being synthesized and characterized. These compounds include linear, layered, and three-dimensional materials. The phosphonate group may contain functional groups prior to reaction with the metal, or to be functionalized after the reaction, providing this flexibility the opportunity to design compounds with specific properties. Several transition metal complexes with a variety of functionalized phosphonic acids were reported in the literature, such as $H_2O_3PCH_2OH$ [1], $H_2O_3PCH_2NH_2$ [2], $H_2O_3PCH_2CH_2NH_2$ [3], $H_2O_3PCH_2N(CH_2\text{–}COOH)_2$ [4], $H_2O_3PCH_2CH_2NC_5H_5$ [5], $H_2O_3PCH_2C(O)NH_2$ [1], $H_2O_3PCH_2NHCH_2COOH$ [6], or $H_2O_3PCH_2CO_2H$ [7], but perhaps the most studied of functionalized phosphonic acids is 2-carboxyethilphosphonic acid, $H_2O_3PCH_2CH_2CO_2H$. There have been published complexes of this ligand with representative metals [8], transition metals [9], and lanthanides [10]. In addition, recently, some materials including a second ligand (excluding water molecules) as 4,4′-bipyridine [9], aniline [11], oxalate anion [12], 2,2′-bipyridine [13], or 1,10-phenanthroline [14], have been reported.

The synthesis of compounds containing more than one ligand is much more difficult to control, and experimental synthesis conditions play a fundamental role. *A priori* both the final stoichiometry and the structure of the complexes are strongly determined by several factors [15], such as the molar ratio of reagents, pH, counteranion, versatily of the central metal coordination geometry, solvents used [16], or temperature and time of reaction (thermodynamic or kinetic control) [17], the design of a synthetic route being very important for obtaining compounds with singular structures and, therefore, with specific properties [18]. Moreover, the presence of aromatic rings allows the existence of π–π stacking interactions, which may involve the formation of more complicated supramolecular networks [15] even though some works indicate that the behavior of aromatic ligands as 2,2′-bipyridine and 1,10-phenanthroline should be similar, acting both exclusively as bidentate chelating ligands, and reducing the formation of high dimensional structures [19].

The complexity of the aspects stated above can be very well exemplified by the known complexes with 2-carboxyethilphosphonic

* Corresponding author.
E-mail address: jrgm@uniovi.es (J.R. García).

0022-4596/$ - see front matter © 2011 Elsevier Inc. All rights reserved.
doi:10.1016/j.jssc.2011.10.003

Table 1
Synthesis conditions (molar ratio of reagents, final pH, temperature and reaction time).

	Metal	1,10-Phenanthroline	2-Carboxyethylphosphonic acid	H_2O	pH	T (K)	Time (h)	Reference
Mn	1	1	1	2.07	–	433	72	[45]
Cu	1	1	1	0.39	–	433	120	[46]
Zn	1.2	1	1	0.39	–	423	96	[47]
Cd	1	1.2	1	0.78	~11	433	144	[48]
Co	1	1	1	0.55	~5	408	48	This work
Cu	1	1	1	0.55	~5	408	48	This work
Cd	1	1	1	0.55	~5	408	48	This work

acid, and 2,2′-bipyridine or 1,10-phenanthroline as ligands. The compounds of Mn [13], Co [20], or Zn [21] with 2-carboxyethilphosphonic acid and 2,2′-bipyridine, obtained in similar (but no identical) experimental conditions are isostructurals, crystallizing as single centrosymmetric dimers with very similar unit cell parameters. In contrast, the combination of 2-carboxyethilphosphonic acid and 1,10-phenanthroline produced four structure-types with four different metals, Mn [22], Cu [23], Zn [24], and Cd [14]. In these cases, the experimental conditions are sensibly different for every structure.

Considering these results, our research focuses on the synthesis of compounds with different transition metals, in diverse experimental conditions (molar ratio, temperature, time, etc.), with 2-carboxyethilphosphonic acid and 1,10-phenanthroline, in order to analyze the influence of ligands, the coordination capacity and nature of the metal, and the synthesis conditions, on the formation of the final framework.

In this work, the synthesis, crystal structure, and both thermal and magnetic characterization of two novel metal transition complexes based on the divalent metals cobalt and cadmium are described. For a third compound based on copper(II), previously reported at room temperature [23], crystal structure at low temperature (120 K), and thermal and magnetic characterization are also reported. The synthesis and crystallization conditions were the same for our three compounds, and different from the published structures (see Table 1). This results show the versatility of 2-carboxyethilphosphonic acid to increase the dimensionality of the crystal lattice, and the existence of different interactions in each of the three structures to yield the 3D framework. On the other hand, to the best of our knowledge, this is the first magnetic study published for this kind of compounds.

2. Experimental section

2.1. Materials and methods

All the reagents were used as commercial sources with no further purification. All aqueous solutions were prepared with distilled water. On samples previously weighed in a Perkin-Elmer AD-2Z microbalance, the C–H–N quantitative determination was obtained by using a Perkin-Elmer 2400 elemental analyzer. The IR spectra for the three compounds were recorded on a UV–VIS–NIR Perkin Elmer Lambda 900 spectrometer in the region from 4000 to 600 cm^{-1}. A Mettler-Toledo TGA/SDTA851e was used for the thermal analyses in oxygen dynamic atmosphere (50 mL/min) at a heating rate of 10 °C/min. In all cases, ca. 10 mg of powder sample was thermally treated, and blank runs were performed. Powder X-ray diffraction (PXRD) data for compounds **1** and **3** were collected, at 298 K, in transmission mode, on an Oxford Diffraction Gemini S using mirror-monochromated Cu$K\alpha$ radiation (λ=1.5418 Å) and a Ruby CCD area detector. The powder patterns were collected using three 2θ detector positions (−82°, 0°, and 82°). For each detector position the sample was rotated 300° on ϕ, with 300 s for each rotation and, finally, the integrated data was averaged on the 2θ range 6–60°. Peak intensities were integrated over the whole ring in step-scan mode, with a step size of 0.04° and 0.03°, respectively. For compound **2**, the X-ray powder diffraction patterns were performed on a Seifert XRD 3000 T/T XRPD diffractometer in a 2θ range of 5–50°, with a step size of 0.025°. DC magnetic susceptibility measurements of powdered samples were performed using Quantum Design PPMS magnetometer whilst heating from 2 to 300 K under an applied magnetic field of strength 1 kOe. Magnetization as a function of field (H) was measured using the same magnetometer in the $-85 \leq H/\mathrm{kOe} \leq 85$ at 2 K after cooling the sample in zero field.

2.2. Synthesis

$Cu_2(HO_3PCH_2CH_2COO)_2(C_{12}H_8N_2)_2(H_2O)_2$ (**1**), $[Co_2(HO_3PCH_2CH_2COO)_2(C_{12}H_8N_2)_2(\mu\text{–}OH_2)](H_2O)$ (**2**), and $Cd_2(HO_3PCH_2CH_2COO)_2(C_{12}H_8N_2)_2$ (**3**) were synthesized under the same hydrothermal conditions. For the preparation of **1**, 0.195 g (1 mmol) of $Cu(CH_3COO)_2 \cdot H_2O$ [Prolabo], 0.150 g (1 mmol) of 2-carboxyethylphosphonic acid [Aldrich], and 0.176 g (1 mmol) of 1,10-phenanthroline [Prolabo] were mixed in 10 mL of distilled water. The reaction mixture was stirred at room temperature to homogeneity, then placed in a Teflon-lined stainless vessel (40 mL) and heated to 408 K for 48 h under autogenous pressure and afterwards cooled slowly to room temperature. Compounds **2** and **3** were obtained with a synthesis procedure analogous by using 0.207 g (1 mmol) of $Co(CH_3COO)_2$ [Probus], or 0.260 g (1 mmol) of $Cd(CH_3COO)_2 \cdot 2H_2O$ [Merck], respectively. In all cases, the resulting products were obtained as unique phases of single-crystals, blue for the Cu-complex, red for the Co-complex, and colorless for the Cd one. The solids were filtered off, washed thoroughly with distilled water, and finally air-dried at room temperature.

2.3. Single-crystal X-ray diffraction

Data collection was performed on an Oxford Diffraction Gemini S single-crystal diffractometer, using mirror-monochromated radiation. Images were collected at a 55 mm fixed crystal–detector distance, using the oscillation method, with variable exposure time per image. **1** was measured at 120 K, using Mo$K\alpha$ radiation (λ=0.71073 Å). **2** was measured using Cu$K\alpha$ radiation (λ=1.5418 Å) at 120 and 293 K. Finally, **3** was measured at 293 K, using also Cu$K\alpha$ radiation. The crystal structures were solved by direct methods and refined by full-matrix least squares on F^2. All non-H atoms were anisotropically refined, while H atoms were either geometrically placed or obtained from the difference Fourier map and refined riding on their parent atoms, with fixed isotropic displacement parameters. The geometrically placed hydrogen atoms were: for **1** only H30, for **2** only H7 (for both temperatures), and for **3** all H atoms. Crystallographic calculations were carried out using the following programs: CrysAlis CCD for data collection, CrysAlis RED for cell refinement, data reduction

Table 2
Crystal data and structure refinement using a method based on a full-matrix least squares on procedure and using empirical absorption corrections.

Compound	**1** (120 K)	**2** (120 K)	**2** (293 K)	**3** (293 K)
Formula	$C_{30}H_{30}Cu_2N_4O_{12}P_2$	$C_{30}H_{28}Co_2N_4O_{11}P_2 \cdot H_2O$	$C_{30}H_{28}Co_2N_4O_{11}P_2 \cdot H_2O$	$C_{30}H_{30}Cd_2N_4O_{10}P_2$
Formula weight (g mol^{-1})	827.62	818.38	818.38	889.30
Temperature (K)	120(2)	120(2)	293(2)	293(2)
Wavelength	Mo$K\alpha$ (0.71073 Å)	Cu$K\alpha$ (1.5418 Å)	Cu$K\alpha$ (1.5418 Å)	Cu$K\alpha$ (1.5418 Å)
Crystal system	Triclinic	Orthorhombic	Orthorhombic	Triclinic
Space group	*P-1*	*Pbcn*	*Pbcn*	*P-1*
Unit cell dimensions				
a (Å)	7.908(5)	21.1057(2)	21.1956(2)	8.162(5)
b (Å)	10.373(5)	9.8231(1)	9.8916(1)	9.500(5)
c (Å)	11.515(5)	15.4251(1)	15.4139(2)	11.148(5)
α (°)	111.683(5)	90	90	102.623(5)
β (°)	95.801(5)	90	90	98.607(5)
γ (°)	110.212(5)	90	90	113.004(5)
Cell volume (Å^3)	794.9(7)	3197.98(5)	3231.65(6)	749.4(7)
Z	1	4	4	1
Calc. density (mg m^{-3})	1.729	1.700	1.682	1.971
Absorption coefficient (mm^{-1})	1.511	9.708	9.607	12.971
F(0 0 0)	422	1672	1672	440
Crystal size (mm^3)	0.1046 × 0.0714 × 0.0297	0.1973 × 0.1395 × 0.1191	0.1973 × 0.1395 × 0.1191	0.0995 × 0.0782 × 0.0199
Theta range for data collection (°)	3.29–30.85	3.55–70.46	3.54–70.49	4.21–70.73
Index ranges	$-11 \le h \le 10$, $-10 \le k \le 14$, $-14 \le l \le 16$	$-25 \le h \le 18$, $-5 \le k \le 12$, $-17 \le l \le 18$	$-25 \le h \le 19$, $-11 \le k \le 12$, $-18 \le l \le 17$	$-9 \le h \le 8$, $-11 \le k \le 11$, $-11 \le l \le 13$
Reflections collected	6701	7829	12408	5775
Independent reflections	4413 [R_{int}=0.04]	2994 [R_{int}=0.02]	3094 [R_{int}=0.03]	2765 [R_{int}=0.04]
Completeness to θ=70°	99.6%	98.4%	99.6%	99%
Max. and min. transmission	0.956 and 0.881	0.315 and 0.246	0.318 and 0.250	0.773 and 0.340
Data/restraints/parameters	4413/0/269	2994/1/286	3094/1/286	2765/0/218
Goodness-of-fit on F^2	0.811	1.028	1.075	1.073
Final R indices [$I > 2\sigma(I)$]	$R1$=0.0441, $wR2$=0.0600	$R1$=0.0310, $wR2$=0.0843	$R1$=0.0306, $wR2$=0.0797	$R1$=0.0335, $wR2$=0.0887
R indices (all data)	$R1$=0.0859, $wR2$=0.0654	$R1$=0.0367, $wR2$=0.0861	$R1$=0.0340, $wR2$=0.0818	$R1$=0.0376, $wR2$=0.0905
Largest diff. peak and hole	0.452 and −0.476 e Å^{-3}	0.295 and −0.841 e Å^{-3}	0.268 and −0.694 e Å^{-3}	0.404 and −1.023 e Å^{-3}

and empirical absorption correction [25], SIR-92 for structure solution [26], SHELXL-97 for structure refinement and prepare materials for publication [27], PLATON and PARST [28] for the geometrical calculations, and ORTEP [29], Mercury [30] and Diamond [31] for molecular graphics. Crystal data and structure refinement details for the three compounds are given in Table 2, while the selected bond lengths and bond angles, and hydrogen bonds for all compounds are listed in Tables 3 and 4, respectively.

3. Results and discussion

3.1. Description of crystal structures

The structure of $Cu_2(HO_3PCH_2CH_2COO)_2(C_{12}H_8N_2)_2(H_2O)_2$ (**1**) has been previously described at room temperature in the literature [23]. The dimeric structure is formed by two copper(II) cations, two 2-carboxyethylphosphonate anions, two phenanthroline molecules, and two coordinated water molecules. Every copper atom is five-coordinated in a square-pyramidal geometry by one oxygen atom of a phosphonate group, one oxygen atom of a carboxylate group, the oxygen atom of a coordinated water molecule, and the two nitrogen atoms of a phenanthroline molecule (Fig. 1). In the crystal packing, the dimers are linked by strong hydrogen bonds (O3–H30···O2) forming chains along *b*-axis, and by hydrogen bonds (O6–H6B···O4) between chains along *a*-axis giving rise to the layer structure.

The phenanthroline molecules seem to play an important role in the final crystal structure (aspect not included in the previous study [23]). They become parallel to each other, with a short distance between adjacent phenanthroline planes of 3.58(1) Å, which is within the range to consider the establishment of strong π–π stacking interactions between aromatic ligands [32]. The existence of C–H···π interactions were also analyzed, but the parallel disposition of the phenanthroline rings in the crystal structure does not allow us to determine these interactions in this case.

At 120 K the geometry of the complex is the same, with differences in the distances of metal–ligand bond lower than 0.1 Å, and with variations below 3° for the angles. The hydrogen bond network is also the same (Table 4). Intramolecular O6–H6A···O2 and intermolecular O3–H30···O2 hydrogen bonds hardly change, but O6–H6B···O4 becomes shorter (1.91 Å vs. 2.19 Å at room temperature), due to a more favorable orientation of the H6B atom (the D–H···A angle is now 171° vs. 129° at room temperature). The π–π stacking is also favored by decreasing temperature, and the distance between phenanthroline planes decreased to 3.52(1) Å. As expected, collecting data at lower temperature produces cell shrinks, but the corresponding decrease of cell parameters is not symmetric. The *b*-axis remains constant, what can be explained by the presence of the hydrogen bond O3–H30···O2, which does not change significantly with temperature, while the *a*-axis shows a small variation, which could be related to the difference in the strength of the O6–H6B···O4 hydrogen bond at both temperatures, previously indicated.

For $[Co_2(HO_3PCH_2CH_2COO)_2(C_{12}H_8N_2)_2(\mu\text{–}OH_2)](H_2O)$ (**2**), single-crystal XRD data were collected at room (293 K) and low temperature (120 K), with no significant changes observed between them (Table 2). The supramolecular structure is formed by units (Fig. 2) consisting of two cobalt(II) ions linked with two bidentate carboxylate (*syn–syn* bridging mode) in *cis*

arrangement, forming an eight-membered ring, two molecules of phenanthroline (mutually perpendicular, with an angle of 86°), and one water-bridge molecule. Each cobalt(II) ion is six-coordinated (with pseudo-octahedral geometry) by one phosphonate oxygen atom (O1), two carboxylate oxygen atoms (O4 and O5), one water-bridge oxygen atom (O6), and the two nitrogen atoms of a phenanthroline molecule. A selected list of bond lengths and angles is shown in Table 3. These units are linked by the phosphonate ligand forming chains (Fig. 3) and channels along *c*-axis, where the free water molecules are placed. Calculation by PLATON indicates that these channels represent the 3.9% of the crystal volume. The structure of complex **2** is stabilized by strong O–H···O hydrogen bonds, with the phosphate oxygen O2 acting always as acceptor (Table 4). It is intramolecularly bonded with the water bridge molecule O6, and intermolecularly with the O3 phosphate oxygen of a neighboring molecule of the chain. Furthermore, the arrangement of water molecules in the channels along *c*-axis is also stabilized by the hydrogen bond O7–H7···O2. The chains structure is extended into a 3D framework through the π–π stacking interactions between partially overlapped adjacent phenanthroline rings (Fig. 3) with interplanar distance of 3.38 Å at 293 K (3.35 Å at 120 K). The extension of the structure along *a*- and *b*-axes is given jointly by the aforementioned orientation of the two phenanthroline molecules in the structural unit, which foster π–π interactions in two directions almost perpendicular, matching with these two crystallographic axes. No reliable C–H···π interactions were found.

When the temperature is increased the *c*-axis maintains almost constant its magnitude (Table 2). This result could be explained taking into account the strong hydrogen bond between neighboring phosphonate groups in the chains along *c*-axis, O3–H30···O2, that presents the same values at both temperatures. The increasing of temperature also influences the position of the free water in the channels: the molecule has a higher thermal displacement and the distance of the hydrogen bond with the oxygen atom of the neighboring phosphate group increases (see Table 4).

Compound $Cd_2(HO_3PCH_2CH_2COO)_2(C_{12}H_8N_2)_2$ (**3**) crystallizes in the triclinic system, in space group *P-1* (Table 2). Every cadmium(II) ion is six-coordinated with distorted octahedral geometry by two nitrogen atoms of a phenanthroline molecule (N1 and N2), and four oxygen atoms: two carboxylate oxygen atoms (O4 and O5), and two phosphate oxygen atoms (O2 and O2′), belonging to two different 2-carboxyethylphosphonic acid ligands. These phosphate oxygen atoms act like bridges, connecting the two metals with an angle of 101.7(1)°, and forming structural units with two cadmium atoms, two phenanthroline molecules, and two 2-carboxyethylphosphonate ligands (Fig. 4). A selected list of bond lengths and angles is shown in Table 3. These units are linked via phosphonate bridges forming chains along *a*-axis. These chains are assembled by strong intermolecular hydrogen bonds O1–H11···O3 (Table 4) along *b*-axis, constituting a 2D layer (Fig. 5), which is extended into a final 3D structure by aromatic π–π stacking interactions between face-to-face phenanthroline molecules of intercalated layers, with interplanar distance of 3.43 Å (Fig. 6). Also appear C–H···π interactions between the two hydrogen atoms of C14 and the neighboring phenanthroline molecules (d= 3.23 Å and 3.27 Å and A=112° and 109° in the C–H···π patterns; d and A stand for the H···π separations and C–H···π angles in the C–H···π patterns, respectively) that help to stabilize the 3D framework (Figs. 4 and 6).

Table 3
Selected bond lengths (Å) and bond angles (degrees) for the compounds **2** and **3**.

	Bond lengths (Å)			Bond angles (°)	
Compound 2	**120 K**	**293 K**		**120 K**	**293 K**
Co1–O1	2.049(2)	2.055(1)	O1–Co1–O4	172.64(7)	172.61(7)
Co1–O4	2.030(2)	2.030(2)	O1–Co1–O5	94.20(6)	94.51(6)
Co1–O5	2.076(2)	2.072(2)	O1–Co1–O6	86.08(6)	85.86(5)
Co1–O6	2.229(1)	2.239(1)	O1–Co1–N1	86.45(7)	86.54(6)
Co1–N1	2.125(2)	2.131(2)	O1–Co1–N2	87.72(6)	87.99(6)
Co1–N2	2.173(2)	2.176(2)	O4–Co1–O5	93.08(7)	92.70(7)
Co1–Co1	3.697(1)	3.705(1)	O4–Co1–O6	92.62(6)	92.32(6)
			O4–Co1–N1	94.62(7)	95.00(7)
			O4–Co1–N2	85.41(7)	85.31(7)
			O5–Co1–O6	91.59(6)	91.69(6)
			O5–Co1–N1	90.34(7)	90.71(6)
			O5–Co1–N2	167.46(7)	167.52(7)
			O6–Co1–N1	172.40(7)	172.19(6)
			O6–Co1–N2	100.91(6)	100.69(6)
			N1–Co1–N2	77.40(7)	77.23(7)
			Co1–O6–Co1	112.1(1)	111.68(9)
Compound 3	**293 K**			**293 K**	
Cd–O2	2.264(3)		O2–Cd–O2′	78.3(1)	
Cd–O2′	2.299(3)		O2–Cd–O4	90.7(1)	
Cd–O4	2.376(3)		O2′–Cd–O4	94.1(1)	
Cd–O5	2.328(4)		O2–Cd–O5	142.6(1)	
Cd–N1	2.352(3)		O2′–Cd–O5	88.3(1)	
Cd–N2	2.327(4)		O2–Cd–N1	95.5(1)	
Cd–Cd	3.540(1)		O2′–Cd–N1	92.7(1)	
			O2–Cd–N2	102.9(1)	
			O2′–Cd–N2	164.49(1)	
			O4–Cd–O5	55.2(1)	
			O4–Cd–N1	171.6(1)	
			O4–Cd–N2	101.3(1)	
			O5–Cd–N1	120.2(1)	
			O5–Cd–N2	99.1(1)	
			N1–Cd–N2	71.8(1)	
			Cd–O2–Cd	101.7(1)	

Table 4
Hydrogen bonds.

D–H···A	d(D–H) (Å)		d(H···A) (Å)		d(D···A) (Å)		(D–H···A) (°)	
Compound 1_120 K								
O6–H6A···O2*	0.84(4)		1.90(4)		2.734(4)		171(3)	
O6–H6B···O4[a]	0.86(3)		1.91(3)		2.761(3)		171(3)	
O3–H30···O2[b]	0.82(2)		1.771(2)		2.573(3)		165.8(2)	
Compound 2_	**120 K**	**293 K**	**120 K**	**293 K**	**120 K**	**293 K**	**120 K**	**293 K**
O3–H30···O2[c]	0.84(4)	0.84(4)	1.76(4)	1.77(4)	2.586(2)	2.594(2)	169(4)	170(4)
O6–H60···O2	0.82(4)	0.91(3)	1.92(4)	1.85(3)	2.731(2)	2.745(2)	170(4)	166(3)
O7–H7 ···O2	0.93(3)	0.93(2)	2.12(3)	2.22(3)	3.035(3)	3.057(4)	166(2)	150(2)
Compound 3_293 K								
O1–H11 ···O3[d]	0.820(0)		1.754(1)		2.545(1)		161.52(4)	

Symmetry codes: [a] $-x+1, -y, -z$; [b] $-x+1, -y+1, -z$; [c] $-x, -y+1, -z+1$; [d] $-x+2, -y+1, -z+2$.

* For compound **1**, O6 (the water-bridge molecule's oxygen) corresponds with O1w of the published structure [48].

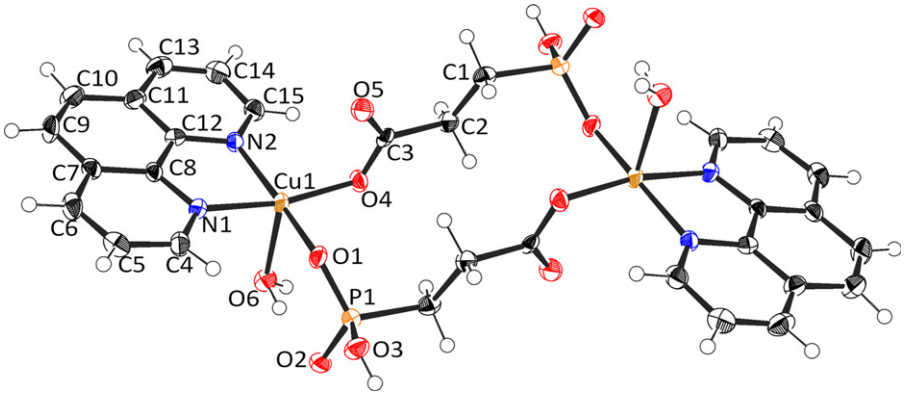

Fig. 1. Asymmetric unit of compound **1**.

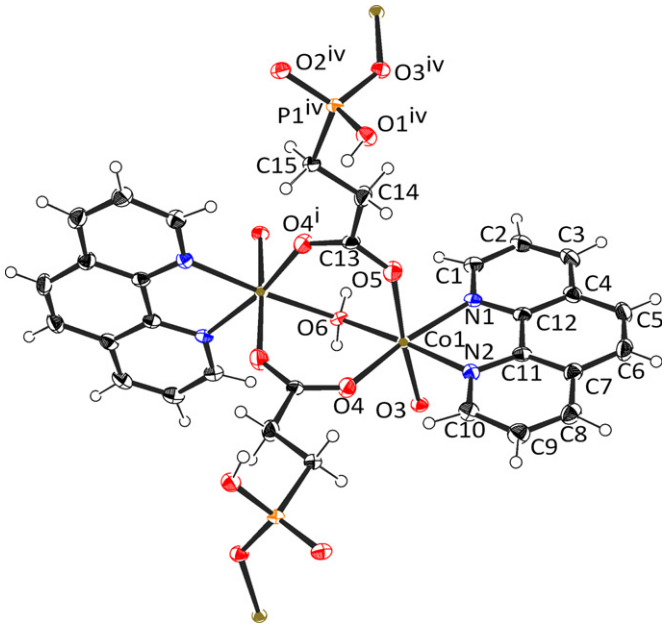

Fig. 2. Asymmetric unit of compound **2**.

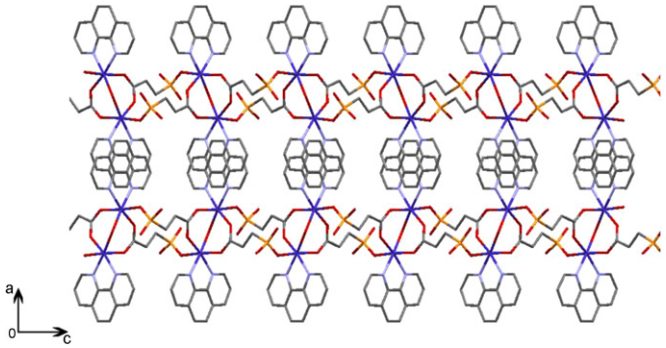

Fig. 3. Structural scheme for compound **2**, showing the union of the units *via* phosphonate ligands, forming chains along *c*-axis. Hydrogen atoms have been omitted for clarity.

3.2. Comparative structural study

From the synthetic point of view, several aspects must be highlighted, mainly the fact that three completely different structures have been obtained starting from identical reaction and crystallization conditions (Table 1). This result becomes more interesting when we consider the aforementioned transition metal structures with 2-carboxyethylphosphonic acid and 2,2′-bipyridine (see introduction), or the compounds with 1,10-phenanthroline and dicarboxylic acids as CO_2–$(CH_2)_n$–CO_2, which crystallize isostructural, as centrosymmetric dimer molecules: Mn and Cd with CO_2–$(CH_2)_2$–CO_2 [33]; Mn, Co, and Zn with CO_2–$(CH_2)_4$–CO_2 [34]; and Zn and Co with CO_2–$(CH_2)_6$–CO_2 [35]. Similarly, compounds of Mn, Co, and Zn with 1,10-phenanthroline and phosphoric acid [36] are also isostructural, and also appear crystallizing as dimers.

On the other hand, the crystal structures of Co and Cd shown in this work are different from those already known from Cd and Mn compounds, leading us a total of six different structures with transition metals and only two ligands. To the best of our knowledge, this behavior was not previously reported for similar ligands. Finally, in the case of Cu, the reaction time or temperature seem not to influence the final compound for a particular ratio of reactants. So it looks that the final structure for this type of compounds under theconditions quoted above can be mainly conditioned by the nature of central metal.

From a structural point of view, the 2-carboxyethylphosphonic acid binds differently to each metal, leading to different frameworks. In structures **1**–**3**, phosphate group remains always protonated, and links to the metal by only one of its oxygen. This behavior also occurs for Zn [24] and Cd [14] published structures, but not for Mn [22]. The fact that the published structure of Cd has been obtained at pH∼11 and the corresponding with Mn at pH∼5 suggests that the protonation of the phosphate group (and therefore how it links to the metal) is independent of pH. Concerning to the acid group, when the metal binds to two oxygen atoms (Co or Cd), the structure consists of chains, while in the opposite case there are discrete structural units, independently of the central atom coordination (five for Zn and Cu, and six for Mn).

As expected, phenanthroline rings play an important role in the formation of 2D layers and 3D supramolecular networks. In compounds **1** and **3** and in the previously published manganese complex [45], the two phenanthroline molecules of the structural unit are oriented in parallel, allowing π–π stacking interactions only along one direction: parallel to *a*-axis for **1**, and on the diagonal to *ab*-plane for **3** and Mn. A similar behavior is found in the crystal of Zn, with π–π stacking interactions between neighboring zwitterions (not shown in Ref. [24]) with distance 3.53 Å, forming layers along *b*-axis. Finally, as discussed previously, the phenanthroline rings in compound **2** stabilize the framework along two axes of the crystal, thanks to its almost perpendicular orientation in the structural unit.

The dimer of compound **1** is very similar to that obtained with 1,10-phenanthroline and succinic acid, so it can be said that, for Cu, 2-carboxyethylphosphonic acid behaves in a similar way to

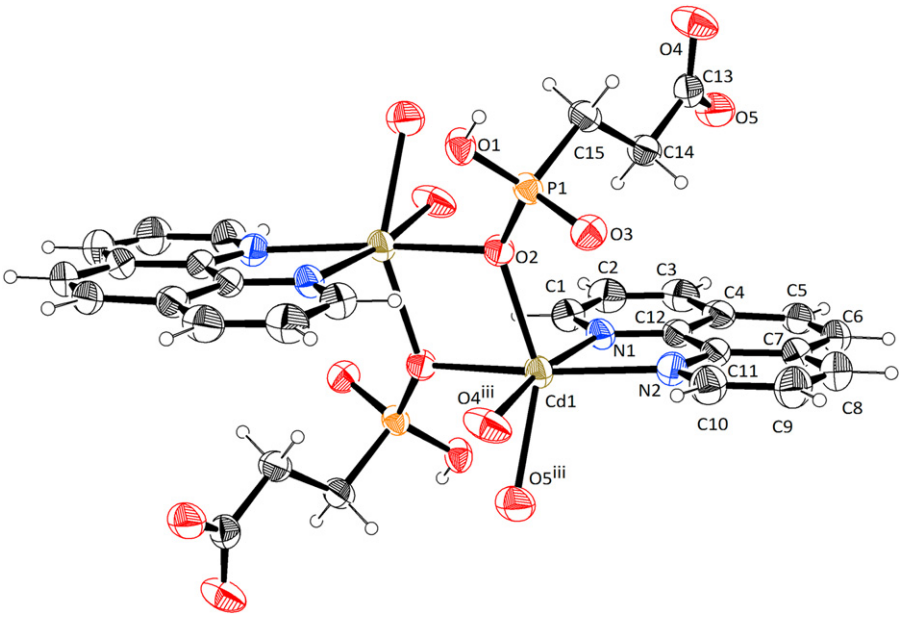

Fig. 4. Asymmetric unit of compound **3**.

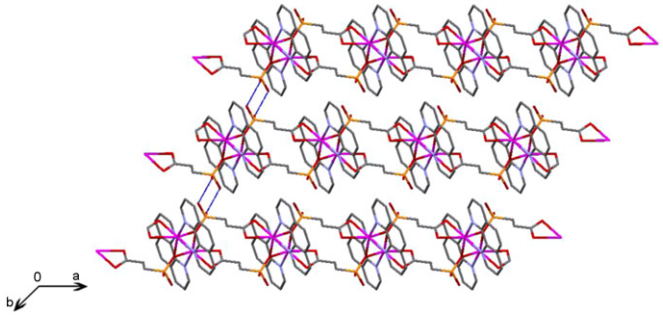

Fig. 5. Packing diagram of compound **3** with a view of the phosphonate chains along *a*-axis and the hydrogen bonds along *b*-axis. Hydrogen atoms have been omitted for clarity.

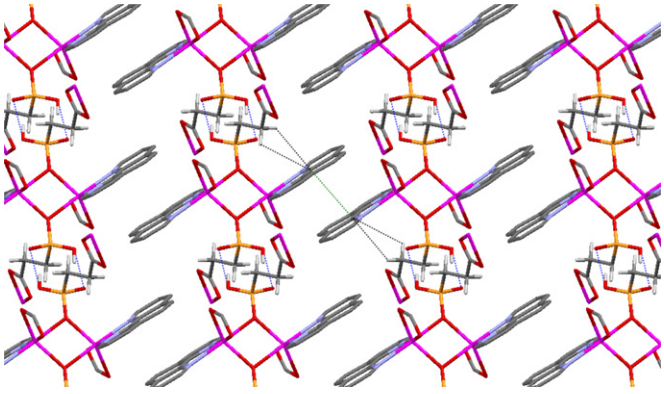

Fig. 6. Packing diagram of compound **3** with a view of π–π stacking interactions between face-to-face phenanthroline molecules, and C–H···π interactions. Hydrogen atoms not involved in the interactions have been omitted for clarity.

the CO_2–$(CH_2)_2$–CO_2. Although its structure has been previously described at room temperature [23], low temperature resolution has allowed determining the influence of hydrogen bonds in the variations of cell parameters with temperature (this information can also be used for studies of atomic volumes [37]).

Compound **2** is the first published complex of Co with 2-carboxyethylphosphonic acid and phenanthroline, and one of the few existing structures [38] with two cobalt atoms linked by a water bridge. Unlike compound **2**, all such structures which include 1,10-phenanthroline [39] are formed by discrete dinuclear units with bridging acid groups forming an eight-membered ring, but in no way forming chains, even in the cases where the ligand is a diacid [15]. Another important point is the fact that none of these five structures have channels that can accommodate small molecules

Compound **3** is different from the complex of Cd already published with those same ligands [14], which present channels with water molecules inside. In the synthesis of both crystals the molar ratio between metal and acid is the same, and the main difference is in reaction times (see Table 1). So that, a priori, structure **3** could be the kinetic control product, while the published one would be the thermodynamic control product. In this regard it is significant that the values of the *a*- and *c*-axes are identical, while the *b*-axis value is double in the published. The coordination environment of Cd in both structures is the same, with equal bond distances. For example, for the Cd–O bonds, average values of 2.352(3) and 2.282(3) Å for the carboxylate and phosphate oxygen atoms, respectively, were found for **3** [against 2.399 and 2.215 Å for the published one] and, for the Cd–N bonds, average distance is 2.340(3) Å [2.337 Å]. The main difference between both structures corresponds to the binding mode of the phosphate groups. In the published structure, the oxygen atom does not form bridges between the metals, leading in a completely different network; while **3** is formed by chains, and the published structure is formed by layers, which define channels where the water molecules are placed. The higher distortion in the octahedral coordination in **3** could facilitate the breaking of a bond to form the published structure.

3.3. IR data

The IR data for compound **1** (Fig. 7a) show the typical broad bands of the coordinated water (centered at 3230 cm^{-1}), while for compound **2** (Fig. 7b) two bands (centered at 3498 and 3554 cm^{-1}) reflect the two types of water molecules in their structure (the last band could be assigned to the O–H stretching vibrations of the hydration water molecule, and the first corresponds to the water-bridge molecule) [39,40]. All the three

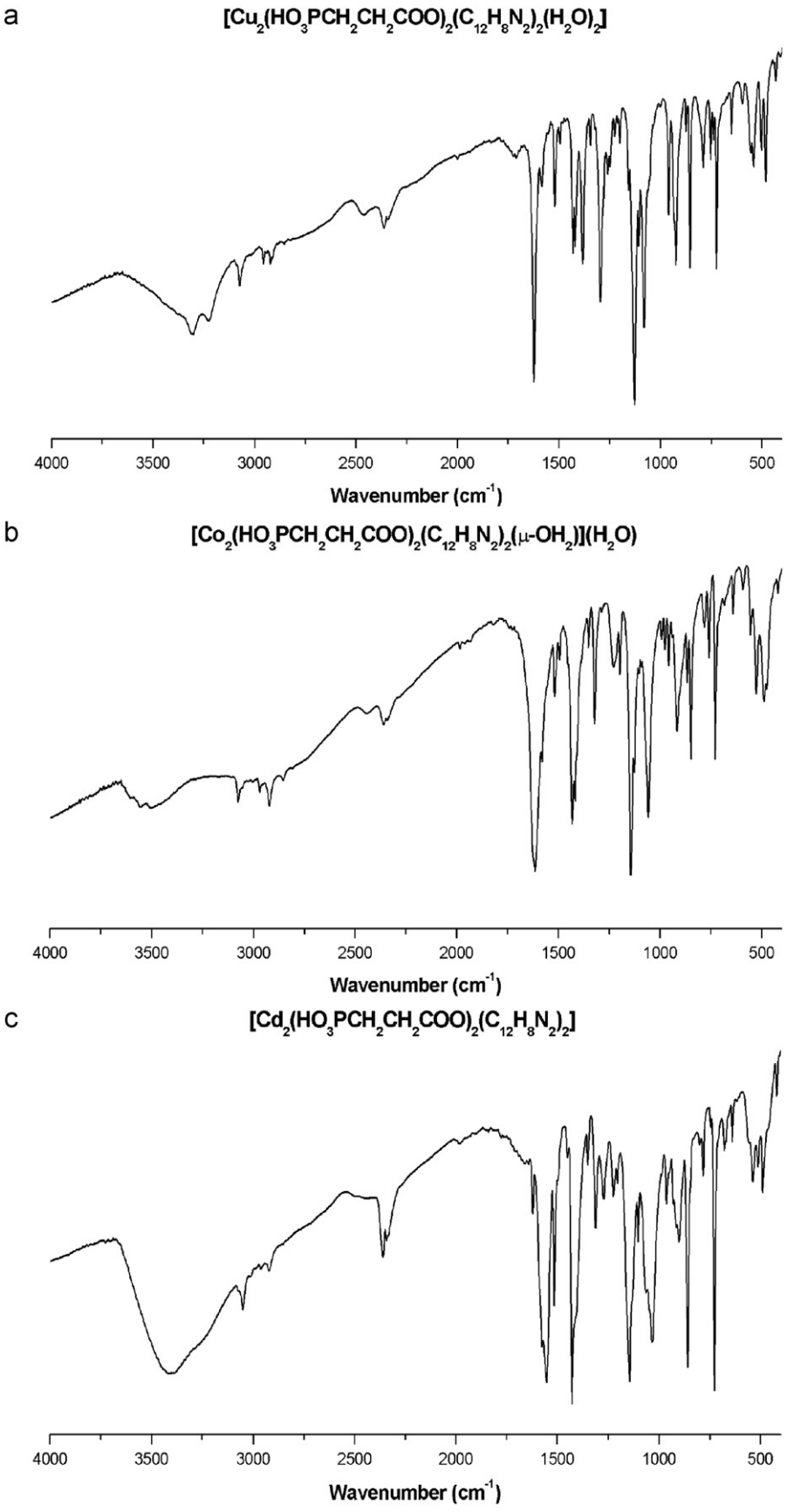

Fig. 7. IR spectra for compounds **1** (a), **2** (b), and **3** (c).

Table 5
Analytical data and weight loss (w.l.) at 1000 °C for the compound synthesized.

Compound	1		2		3	
	Exp.	Calc.	Exp.	Calc.	Exp.	Calc.
%C	43.8	43.54	44.8	44.03	40.7	40.52
%N	7.1	6.77	6.9	6.85	6.6	6.30
%H	3.2	3.65	3.6	3.69	2.6	3.40
%w.l.	64.1	63.63	68.4	64.34	55.5	55.16

compounds show the typical C–H stretching vibrations, of low intensities, close to 2900 cm^{-1}. In the 1400–1730 cm^{-1} region, the υ(C=O) stretching vibrations of the carboxylate/carboxylic groups are located. Compound **1** shows the symmetric and asymmetric vibrations of the carboxylate groups at 1429 and 1622 cm^{-1}, respectively. Similar bands have been also observed in this region for compounds **2** (1430 and 1614 cm^{-1}), and **3** (1427 and 1552 cm^{-1}, Fig. 7c). The absence of a band in the region 1690–1730 cm^{-1} (O–H vibration of –COOH group) is in agreement with a deprotonated carboxy group [41]. Finally, for all these three compounds, the vibrations of the phosphonic group are located at the region 900–1100 cm^{-1} [9].

3.4. Purity of samples

To confirm that the crystal structures are representative of the solids synthesized, XRPD experiments were carried out for **1**–**3**, and the profiles were correlated with the computer-simulated patterns obtained from the single crystal data. Experimental and calculated profiles are shown in Fig. S1 (see Appendix A). The comparative indicates that each of the three samples corresponds to the pure phase, as the elemental analyses (C, H, N) and total weight losses at 1000 °C also confirm (Table 5).

3.5. Thermal stability

The TG/DTG/SDTA curves for all compounds are depicted in Fig. 8. For **1**, the weight loss can be described by three separate and defined steps, with the formation of $Cu_2P_2O_7$ as final product [42]. The first stage, between 25 and 215 °C approximately, associated with a small endothermic peak on the SDTA curve, corresponds to the loss of the two coordinated water molecules [weight loss 4.6% (cal. 4.35%)] in a typical behavior for the water molecules weakly bound to metal [43], characterized for a distance Cu–O (Cu–O6, 2.264 Å) longer than in the case of the carboxyethylphosphonate oxygen atoms (Cu–O1, 1.947 Å or Cu–O4, 1.948 Å). The second step, between 215 and 480 °C approximately, composed by various continuous and overlapping exothermic processes is assigned to the combustion of one phenanthroline molecule [total weight loss 22.3% (cal. 21.78%)] in a analogous behavior to copper complexes with phenanthroline and other organic ligand [43,44]. The third step, between 480 and 780 °C approximately, also associated with a exothermic process and H_2O–CO_2–NO_x evacuation, corresponds to the combustion of the second molecule of phenanthroline and the carboxyethylphosphonate organic fraction [weight loss 37.2% (cal. 37.50%)] and occurs at temperatures slightly higher than those published for the manganese complexes with carboxyethylphosphonate [45], but similar to that of the copper complexes with phenanthroline and other organic ligand.

The thermal behavior of compound **2** is very similar to that described to **1**, with $Co_2P_2O_7$ as decomposition final product [46] and three well differentiated stages. The first (25–275 °C) stage is related to the loss of two water molecules: the free water molecule located in the channels and the bridge water molecule between the cobalt atoms [weight loss 5.1% (cal. 4.40%)]. The low intensity endothermic peak on the SDTA curve indicates that the water molecule placed in the channels can move easily through

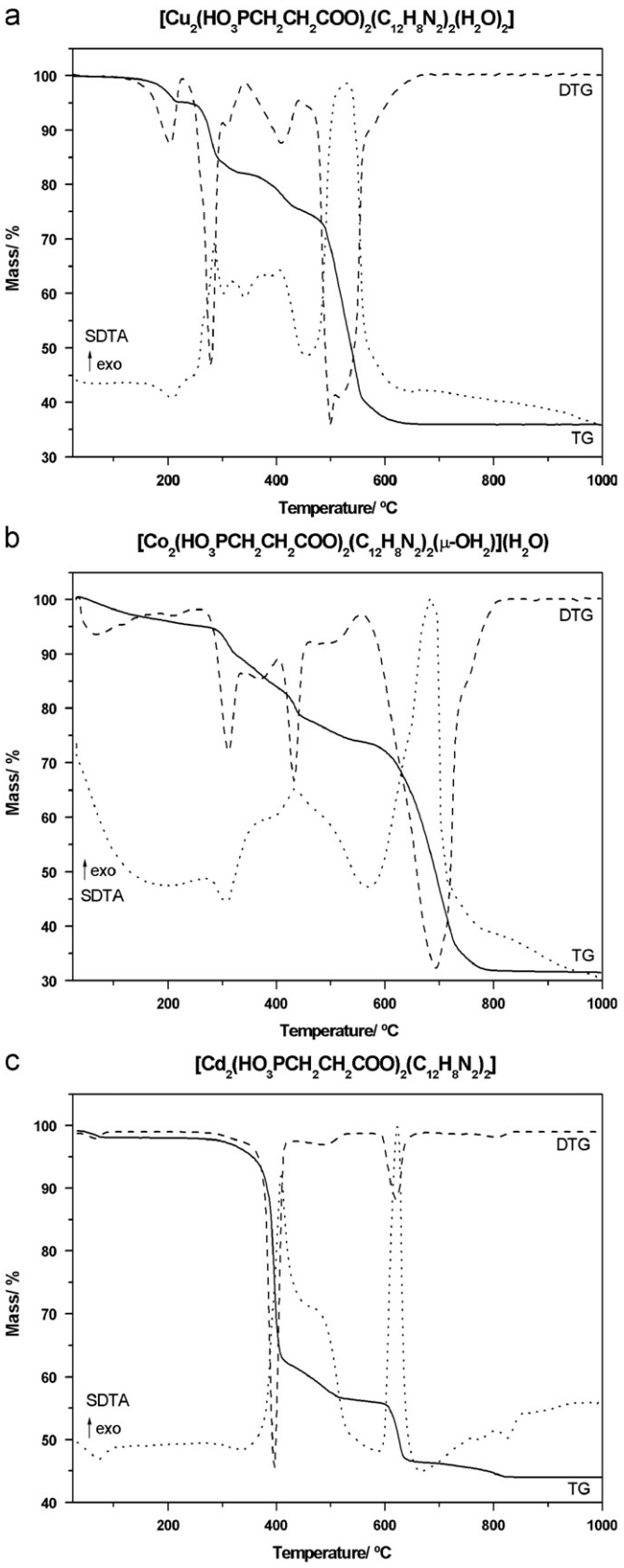

Fig. 8. TG-DTG-SDTA curves for compounds **1** (a), **2** (b), and **3** (c).

them, and the bridge water molecule is weakly bounded to the metallic atoms [43]. Similarly to compound **1**, the distance Co–O is longer in the case of the bridge water molecule (Co–O6, 2.229 Å) than for the carboxyethylphosphonate oxygen atoms (Co–O4, 2.030 Å or Co–O5, 2.076 Å). In a second decomposition range (275–590 °C), with two different steps, the evacuation of one phenanthroline molecule [weight loss 22.2% (cal. 22.00%)] takes place, as is usual for complexes of cobalt with phenanthroline and other organic ligands [45,47]. The first stage corresponds to an endothermic process followed of an exothermic event found at higher temperatures. This means that the partial desorption of the organic matter occurs before the combustion. Later on, to 590–900 °C, the combustion of a second molecule of phenanthroline and the carboxyethylphosphonate organic fraction is observed [weight loss 41.1% (cal. 37.94%)].

Although physisorbed water is detected, compound **3** is anhydrous and consequently their thermal stability is much greater than the previously described for compounds **1** and **2**. Their combustion, in two defined steps, begins to 380°C and concludes to 820 °C with the formation of $Cd_2P_2O_7$ [48]. The first stage corresponds to the combustion of the two phenanthroline molecules [weight loss 40.1% (cal. 40.53%)] and the second one to the carboxyethylphosphonate decomposition and subsequently combustion of the their organic matter [weight loss 15.4% (cal. 14.63%)] in a good agreement with the thermal data reported for others related cadmium compounds [14].

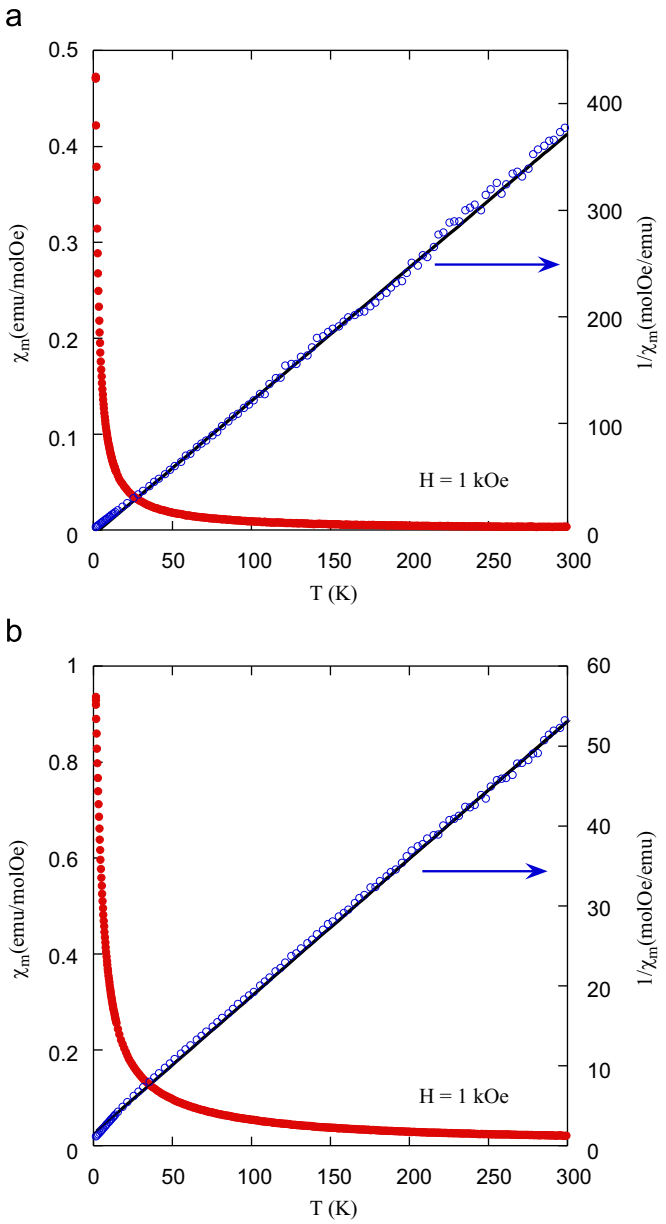

Fig. 9. The temperature dependence of the molar magnetic susceptibility, χ_M (solid points), and its reciprocal magnitude, χ_M^{-1} (empty points), under an applied magnetic field of 1 kOe, for compounds **1** (a) and **2** (b). The solid lines correspond to the Curie–Weiss laws (see text).

3.6. Magnetic study

The magnetic susceptibility of the Cd-based sample (**3**), is negative (not shown), as is expected for a system with all electronic shells filled (Cd^{2+} has an electronic configuration $[Kr]4d^{10}$), showing a Larmor diamagnetic susceptibility, in which the induced magnetic moment is opposite to the applied magnetic field. In contrast, for the Cu- and Co-based samples (**1** and **2**), with partially filled shells, the paramagnetic signal dominates the diamagnetic contribution. These compounds do not show any magnetic long-range order in the measured temperature range between 300 and 2 K. The magnetic susceptibilities are characterized by exhibiting a paramagnetic Curie–Weiss law. The temperature dependence of the molar magnetic susceptibility, χ_M, and its reciprocal magnitude, χ_M^{-1}, for compounds **1** and **2** are depicted in Fig. 9. The Curie constants are estimated from a fit of the temperature dependence of χ_M^{-1} considering all the temperature range investigated, to the Curie–Weiss law (solid line in Fig. 9). The effective paramagnetic moments of Cu^{2+} and Co^{2+} were estimated from these fittings. The magnetic data obtained for the two compounds are gathered in Table 6. The values of the

Table 6
Magnetic data for the compounds **1** and **2** obtained under an applied magnetic field of 1 kOe (C is the Curie constant, θ_P is the paramagnetic temperature, μ_{eff} is the effective paramagnetic moment, and R is the reliability factor of the fitting to the Curie–Weiss law).

Sample	C (cm^3 K/mol)	θ_P (K)	μ_{eff} (μ_B)	R
1	10.03(1)	3.5	1.79(1)	0.9988
2	73.10(2)	−8.8	4.82(1)	0.9997

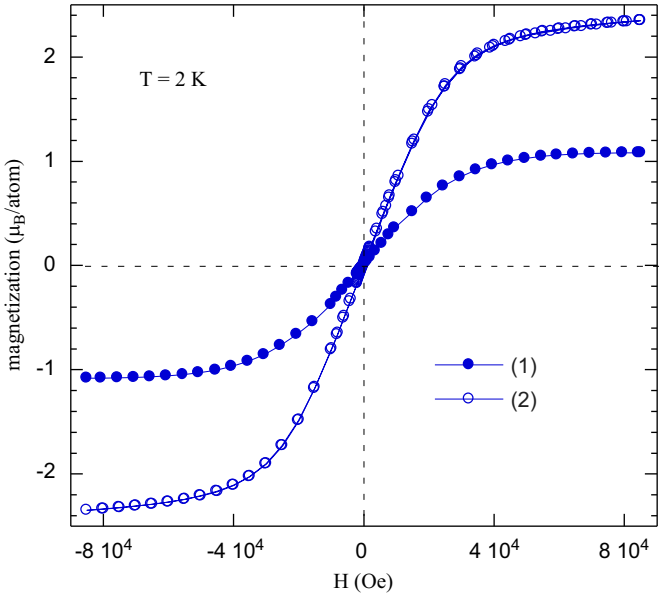

Fig. 10. Magnetization vs. applied magnetic field at 2 K for compounds **1** and **2**.

experimental paramagnetic effective moments 1.79 and 4.82 μ_B shown in the table are quite close to those expected theoretically 1.9 and 4.8 μ_B, for Cu^{2+} ($S=1/2$) and Co^{2+} ($S=3/2$), respectively, assuming that only the spin angular momentum is contributing due to the quenching of the orbital angular momentum.

The dependence of the magnetization with the applied magnetic field at 2 K for compounds **1** and **2** has been represented in Fig. 10. As can be seen, the magnetization in both compounds do not show any ferromagnetic component (no irreversibility in the magnetization curves, $M(H)$). Furthermore, the general shape of the $M(H)$ curves, linear increase at low fields and the tendency to saturation at higher fields, is typical of the Brillouin functions expected in paramagnetic materials. Therefore, the magnetization curves are in good agreement with magnetic susceptibility data. Finally, the values of the magnetization at 85 kOe are ≈ 1.1 μ_B/Cu and 2.4 μ_B/Co for compounds **1** and **2** respectively, which are near from the expected ones for the fully saturated free-ion values (1 μ_B for Cu^{2+} and 3 μ_B for Co^{2+} ions).

4. Conclusions

Metal phosphonates may contain functional groups after their synthesis. This flexibility provides the opportunity to design compounds with tailored properties. This work shows the structural changes induced for a divalent metal in the secondary building units on the $M_2(HO_3PCH_2CH_2COO)_2(C_{12}H_8N_2)_2 \cdot nH_2O$ (M=Cu, Co, Cd) compounds. The cobalt complex is the first published with these two ligands, and the cadmium structure is different from the published, due to the synthesis conditions. The final structure of the complex depends directly on the nature of central metal, but not on its coordination number. The 2-carboxyethylphosphonic acid always appears protonated, regardless of the pH of the synthesis, and the structural unit of the complex is determined by the atoms with which is bonded to metal. In the copper case, discrete units of dimeric form are formed, while for cadmium and cobalt chains are built through the 2-carboxyethylphosphonic acid. In all three cases, the 3D framework is stabilized by π–π stacking interactions along one or two directions in the crystal and, in the case of cadmium compound, also C–H···π interactions appear. The data collection at two different temperatures for copper and cobalt compounds show that the presence of a strong hydrogen bond keeps one cell axis constant. Thermal behavior is related to their structural features, and the three investigated compounds do not show any long-range magnetic order down to 2 K.

Supporting information available

CCDC nos. 830265, 830266, 830267 and 830268 contain the supplementary crystallographic data for compounds described in this article. These data can be obtained free of charge via http://www.ccdc.cam.ac.uk/data_request/cif.

Acknowledgments

We thank financial support from Spanish *Ministerio de Ciencia e Innovación* (MAT2010-15094, MAT2008-06542-C04, MAT2006-01997, *Factoría de Cristalización Consolider Ingenio 2010*) and FEDER. E.F-Z. thanks the *Vicerrectorado de Investigación* of the *Universidad de Oviedo* and the *Banco Santander* for their predoctoral grant.

Appendix A. Supplementary materials

Supplementary materials associated with this article can be found in the online version at doi:10.1016/j.jssc.2011.10.003.

References

[1] G.B. Hix, A. Turner, B.M. Kariuki, M. Tremayne, E.J. MacLean, J. Mater. Chem. 12 (2002) 3220.
[2] C. Fang, Z. Chen, X. Liu, Y. Yang, M. Deng, L. Weng, Y. Jia, Y. Zhou, Inorg. Chim. Acta 362 (2009) 2101.
[3] S. Drumel, P. Janvier, D. Deniaud, B. Bujoli, J. Chem., Soc. Chem. Commun. (1995) 1051.
[4] J.-G. Mao, A. Clearfield, Inorg. Chem. 41 (2002) 2319.
[5] L.A. Vermeulen, R.Z. Fateen, P.D. Robinson, Inorg. Chem. 41 (2002) 2310.
[6] N. Stock, Solid State Sci. 4 (2002) 1089.
[7] A.N. Alsobrook, W. Zhan, T.E. Albrecht-Schmitt, Inorg. Chem. 47 (2008) 5177.
[8] X.-M. Zhang, Eur. J. Inorg. Chem. 43 (2004) 544.
[9] Z. Chen, L. Weng, D. Zhao, Inorg. Chem. Commun. 10 (2007) 447.
[10] F. Serpaggi, G. Férey, Inorg. Chem. 38 (1999) 4741.
[11] S. Drumel, P. Janvier, M. Bujoli-Doeuff, B. Bujoli, J. Mater. Chem. 6 (1996) 1843.
[12] M. Stock, G.D. Stucky, A.K. Cheetham, Chem. Commun. (2000) 2277.
[13] S.-M. Ying, Y. Chen, Q.-Y. Luo, Y.-P. Xv, D.-S. Liu, Acta Cryst. E64 (2008) m166.
[14] X.-M. Zhang, R.-Q. Fang, H.-S. Wu., Cryst. Growth Des. 5 (2005) 1335.
[15] C.-S. Liu, J.-J. Wang, L.-F. Yan, Z. Chang, X.-H. Bu, E.C. Sañudo, J. Ribas, Inorg. Chem. 46 (2007) 6299.
[16] N. Stock, T. Bein, J. Mater. Chem. 15 (2005) 1384.
[17] A.E. Platero-Prats, V.A. de la Peña-O'Shea, D.M. Proserpio, N. Snejko, A. Monge, E. Gutiérrez-Puebla, Acta Cryst. A67 (2011) C95.
[18] A. Clearfield, Curr. Opin. Solid State Mater. Sci. 1 (1996) 268.
[19] X. Xu, Y. Ma, Y. Lu, E. Wang, X. Bai, J. Coord. Chem. 60 (2007) 547.
[20] S.-M. Ying, Y. Chen, J.-Y. Lin, G.-P. Zhou, J.-H. Wu, Acta Cryst. E63 (2007) m2862.
[21] S.-M. Ying, X.-F. Li, W.-T. Chen, D.-S. Liu, J.-H. Liu, Acta Cryst. E63 (2007) m555.
[22] S.-M. Ying, G.-P. Zhou, F. Zhong, J.-Y. Lin, X.-F. Li, Chin. J. Struct. Chem. 28 (2009) 831.
[23] X.-M. Zhang, R.-Q. Fang, H.-S. Wu, S.-W. Ng, Acta Cryst. E59 (2003) m1149.
[24] X.-M. Zhang, R.-Q. Fang, H.-S. Wu, S.-W. Ng, Acta Cryst. E60 (2004) m941.
[25] Oxford Diffraction; CrysAlis CCD and CrysAlis RED. Versions (1.171.34.9) Oxford Diffraction Ltd., Abingdon, Oxfordshire, England, 2009.
[26] A. Altomare, G. Cascarano, C. Giacovazzo, A. Guagliardi, M.C. Burla, G. Polidori, M. Camalli, J. Appl. Cryst. 27 (1994) 435.
[27] G.M. Sheldrick, SHELXS97 and SHELXL97, University of Göttingen, Germany, 1997.
[28] A.L. Spek, J. Appl. Cryst. 36 (2003) 7.
[29] L. Farrugia, J. Appl. Cryst. 30 (1997) 565.
[30] C.F. Macrae, I.J. Bruno, J.A. Chisholm, P.R. Edgington, P. McCabe, E. Pidcock, L. Rodríguez-Monge, R. Taylor, J. van de Streek, P. Wood, Mercury: visualization and analysis of crystal structures, J. Appl. Cryst. 41 (2008) 466.
[31] K. Brandenburg, DIAMOND, Version 3.1, Crystal Impact GbR, Bonn, Germany, 2007.
[32] C. Janiak, J. Chem. Soc. Dalton Trans. (2000) 3885.
[33] Q.W. Wang, X.M. Li, G.G. Gao, L.F. Shi, Acta Cryst. E62 (2006) m3483.
[34] C.F. Ding, S.S. Zhang, M. Zhu, X.M. Li, H. Xu, P.K. Ouyang, Acta Cryst. E61 (2005) m147.
[35] Y.Q. Zheng, Z.P. Kong, Inorg. Chem. Commun. 6 (2003) 478.
[36] Q.L. Li, J.X. Wan, Y.W. Yao, Z. Kristallogr. New Cryst. Struct. 223 (2008) 207.
[37] D.W.M. Hofmann, Acta Cryst. B57 (2002) 489.
[38] F.H. Allen, Acta Cryst. B58 (2002) 380.
[39] F.P. Pruchnik, U. Dawid, A. Kochel, Polyhedron 25 (2006) 3647.
[40] G. Socrates, Infrared and Raman Characteristic Group Frequencies. Tables and Charts, third ed., John Wiley & Sons, Ltd., West Sussex, England, 2004.
[41] A. Distler, S.C. Sevov, Chem. Commun. (1998) 959.
[42] K. Pogorzelec-Glaser, A. Pietraszko, B. Hilczer, M. Polomska, Phase Transition 79 (2006) 535.
[43] F.-Q. Wang, D.-F. Weng, X.-J. Zheng, J.-J. Zhang, H. Ma, L.-P. Jin, Inorg. Chim. Acta 360 (2007) 2029.
[44] B.K. Koo, J. Kim, U. Lee, Inorg. Chim. Acta 363 (2010) 1760.
[45] J.R. Allan, B. McCloy, Thermochim. Acta 214 (1993) 219.
[46] B. El Bali, M. Bolte, Acta Cryst. E58 (2002) i32.
[47] Y.-Q. Zheng, Z.-P. Kong, Inorg. Chem. Commun. 6 (2003) 478.
[48] O.Z. Yesilel, A. Mutlu, C. Darcan, O. Büyükgüngör, J. Mol. Struct. 964 (2010) 39.